PERGAMON

International Journal of Solids and Structures 37 (2000) 7349–7369

INTERNATIONAL JOURNAL OF SOLIDS and STRUCTURES

www.elsevier.com/locate/ijsolstr

On the consistency of viscoplastic formulations

A. Carosio [b], K. Willam [a,*], G. Etse [b]

[a] *CEAE Department, University of Colorado at Boulder, Campus Box 428, Boulder, CO 80309-0428, USA*
[b] *Laboratorio de Estructuras, UNT - CONICET, Av. Independencia 1800, San Miguel deTucumán 4000, Argentina*

Received 16 October 1999; in revised form 31 January 2000

Abstract

A viscoplastic consistency condition is incorporated into the traditional viscoplastic rate format with two objectives in mind: (i) to develop a tangential material operator for rate sensitive behavior similarly to rate independent elastoplasticity, and (ii) to make an analytical reference solution available for evaluating the accuracy of new and well-established computational strategies to integrate the viscoplastic evolution equations.

The viscoplastic tangent operator provides the missing link between rate independent plasticity and rate dependent viscoplasticity. It also furnishes the acoustic tensor, which is required for localization analysis of discontinuous failure. Besides the formulation of the viscoplastic tangent operator, we present an analytical reference solution for perfect J_2 viscoplasticity. This analytical result is subsequently used to determine the accuracy of simplifying assumptions behind the algebraic evaluation of the viscoplastic multiplier, and to quantify the error of the radial return mapping strategy for viscoplastic computations.

Keywords: Consistent viscoplasticity; Localization; Constitutive integration

1. Introduction

In the recent years, novel viscoplastic formulations were proposed, which resemble the mathematical framework of classical elastoplastic flow theory, see Ponthot (1995), Wang et al. (1997), Winnicki et al. (1998). In view of these advances, rate independent plasticity and damage models readily extend to rate dependent material behavior. In addition, well-established elastoplastic strategies may be used to integrate the viscoplastic rate equations based on the algorithmic tangent operator of elastoplasticity (Simo and Taylor, 1985; Ju, 1990).

In the extended formulation, viscoplastic consistency appears in the form of a differential equation, which needs to be solved for the viscoplastic tangent operator that has been missing so far. Thereby, viscoplastic consistency plays the key role to establish continuous transition from plasticity to rate dependent viscoplasticity. An exact solution is presented for small strain J_2 viscoplasticity together with an

* Corresponding author. Fax: +1-303-492-7317.
E-mail address: willam@bechtel.colorado.edu (K. Willam).

0020-7683/00/$ - see front matter
PII: S0020-7683(00)00202-X

error analysis of the closest point projection method (CPPM), which corresponds to the radial return method in case of J_2 plasticity. In addition, the localization properties of the Ducker–Prager viscoplasticity are evaluated for the case of the uniform equibiaxial compression–extension experiment.

2. Consistency of viscoplasticity

The rate dependent flow theory of Bingham solids start from the same assumptions as the flow theory of elastoplasticity. Decomposition of the total strain rate in an elastic and a viscoplastic component

$$\dot{\boldsymbol{\varepsilon}} = \dot{\boldsymbol{\varepsilon}}^{\mathrm{e}} + \dot{\boldsymbol{\varepsilon}}^{\mathrm{vp}} \tag{1}$$

together with the elastic material relation

$$\dot{\boldsymbol{\sigma}} = \boldsymbol{E} : \dot{\boldsymbol{\varepsilon}}^{\mathrm{e}} \tag{2}$$

in which $\boldsymbol{E}$ denotes the elastic material operator and the symbol : indicates a double contraction leads to the standard form

$$\dot{\boldsymbol{\sigma}} = \boldsymbol{E} : (\dot{\boldsymbol{\varepsilon}} - \dot{\boldsymbol{\varepsilon}}^{\mathrm{vp}}). \tag{3}$$

Extending the flow theory of Bingham, the viscoplastic formulation of Perzyna (1966) defines a convex elastic domain $\mathrm{int}(\mathbb{E}_\sigma)$ (Simo and Huges, 1998) in the space of stress and internal variables $\mathrm{int}(\mathbb{E}_\sigma) := \{(\boldsymbol{\sigma}, \boldsymbol{q}) | F(\boldsymbol{\sigma}, \boldsymbol{q}) < 0\}$, where F is a rate independent function of stress and state variables. In the interior of $\mathbb{E}_\sigma$, only elastic loading–unloading processes take place. While elastoplastic flow is confined to the plastic yield surface, $\partial\mathbb{E}_\sigma := \{(\boldsymbol{\sigma}, \boldsymbol{q}) | F(\boldsymbol{\sigma}, \boldsymbol{q}) = 0\}$, viscoplastic flow is associated with states in the exterior of $\mathbb{E}_\sigma$. Thereby, the magnitude of viscoplastic flow is proportional to or a nonlinear function of overstress from $\partial\mathbb{E}_\sigma$, while the direction of viscoplastic flow is governed by the gradient of the viscoplastic potential $Q = Q(\boldsymbol{\sigma}, \boldsymbol{q})$, i.e.

$$\dot{\boldsymbol{\varepsilon}}^{\mathrm{vp}} = \frac{\langle \psi(F) \rangle}{\eta} \boldsymbol{m}, \quad \text{where } \boldsymbol{m} = \frac{\partial Q}{\partial \boldsymbol{\sigma}}. \tag{4}$$

Here, η denotes the viscosity parameter, $\langle\ \rangle$ are the McCauley brackets with $\langle x \rangle = 0.5(x + |x|)$, ψ is an arbitrary dimensionless function of the *over-stress*, usually of the form $\psi(F) = (F/K)^N$ with K normalizing the overstress function. If $Q = F$, the viscoplastic flow is termed associated. As in elastoplasticity, the internal variables are related to the viscoplastic strain, i.e., $\boldsymbol{q} = \boldsymbol{q}(\boldsymbol{\varepsilon}^{\mathrm{vp}})$. A scalar format of the internal variables reduces the isotropic hardening–softening evolution law to $\dot{q} = \boldsymbol{H} : \dot{\boldsymbol{\varepsilon}}^{\mathrm{vp}}$.

In viscoplasticity, the yield condition $F(\boldsymbol{\sigma}, q) > 0$ is an inequality, which distinguishes viscoplastic loading from elastic unloading. There is no restriction on the rate of the yield function, in other words, no viscoplastic consistency condition restricts the inelastic process to satisfy the yield function $F = 0$ under persistent viscoplastic loading. Consequently, a viscoplastic tangent material operator may be constructed only in an algorithmic sense when implicit integration of the viscoplastic process is considered during a finite time step.

2.1. Continuous viscoplasticity

Recently, Ponthot (1995) presented a 'continuous' viscoplastic formulation. He introduced a zero-valued yield condition, $\bar{F}(\boldsymbol{\sigma}, q, \dot{\lambda}) = 0$, from which a consistency condition can be derived under persistent viscoplastic flow when $\dot{\bar{F}} = 0$. This extension of traditional elastoplasticity assumes that the ratio of the overstress function and the viscosity defines the viscoplastic multiplier,

$$\dot{\lambda} = \frac{\psi(F)}{\eta} \quad \text{such that} \quad \dot{\boldsymbol{\varepsilon}}^{\text{vp}} = \dot{\lambda}\boldsymbol{m}, \tag{5}$$

which is controlled by viscoplastic consistency condition. Introducing a rate dependent yield condition in the format

$$\bar{F}(\boldsymbol{\sigma}, q, \dot{\lambda}) = F(\boldsymbol{\sigma}, q) - \psi^{-1}(\dot{\lambda}\eta) = 0, \tag{6}$$

this corresponds to the usual format in elastoplasticity except for the explicit dependence of the resistance function on $\dot{\lambda}$. Loading–unloading leads to the consistency condition of viscoplasticity in the form of $\dot{\lambda}\dot{\bar{F}} = 0$, which assures that the inelastic process satisfies $\bar{F} = 0$ under persistent viscoplastic flow.

The viscoplastic consistency condition expands into

$$\dot{\bar{F}} = \bar{\boldsymbol{n}} : \dot{\boldsymbol{\sigma}} + \bar{r}\dot{\lambda} + \bar{s}\ddot{\lambda} = 0, \tag{7}$$

where

$$\bar{\boldsymbol{n}} = \frac{\partial F}{\partial \boldsymbol{\sigma}}, \tag{8}$$

$$\bar{r} = \left(\frac{\partial F}{\partial q} - \frac{\partial \psi^{-1}(\eta\dot{\lambda})}{\partial q} \right) h, \tag{9}$$

$$\bar{s} = -\frac{\partial \psi^{-1}(\eta\dot{\lambda})}{\partial \dot{\lambda}}, \tag{10}$$

In general, $\psi^{-1} = \psi^{-1}(q)$, i.e., the inverse over-stress function is also a function of the internal variables, which in turn are a function of the viscoplastic strain rate and thus are linear in $\dot{\lambda}$.

$$\dot{q} = h(\boldsymbol{\sigma}, q)\dot{\lambda}. \tag{11}$$

2.2. Consistent viscoplasticity

Using a similar argument Wang (1997) included the rate of state variables as an independent state variable, rendering the viscoplastic yield criterion rate dependent, i.e.,

$$\hat{F} = \hat{F}(\boldsymbol{\sigma}, q, \dot{q}) = 0. \tag{12}$$

As in the previous case, the viscoplastic strain rate follows Eq. (5) and the rate of internal variables Eq. (11). In this case, the viscoplastic consistency condition expands into

$$\dot{\hat{F}} = \hat{\boldsymbol{n}} : \dot{\boldsymbol{\sigma}} + \hat{r}\dot{\lambda} + \hat{s}\ddot{\lambda} = 0, \tag{13}$$

where

$$\hat{\boldsymbol{n}} = \frac{\partial \hat{F}}{\partial \boldsymbol{\sigma}} + \frac{\partial \hat{F}}{\partial \dot{q}} \frac{\partial h}{\partial \boldsymbol{\sigma}}, \tag{14}$$

$$\hat{r} = \left(\frac{\partial \hat{F}}{\partial q} + \frac{\partial \hat{F}}{\partial \dot{q}} \frac{\partial h}{\partial q} \right) h, \tag{15}$$

$$\hat{s} = \frac{\partial \hat{F}}{\partial \dot{q}} h. \tag{16}$$

Comparing Eqs. (7) and (13), the following differential equation holds for both the consistent and the continuous viscoplastic formulations

$$\dot{f} = \boldsymbol{n} : \dot{\boldsymbol{\sigma}} + r\dot{\lambda} + s\ddot{\lambda} = 0, \tag{17}$$

where $\boldsymbol{n}$, r and s have slightly different meanings according to the two formulations, with $f = \bar{F}$ or $f = \hat{F}$.

2.3. Analytical format of the viscoplastic tangent operator

In order to develop an analytical viscoplastic tangent operator, we consider that the solution is known at the stage $t = t_0$ of the rate-dependent process, which serves as initial condition. The tangential linearization of the inelastic process is governed by the elasto-viscoplastic differential expression

$$\dot{\boldsymbol{\sigma}} = \boldsymbol{E} : (\dot{\boldsymbol{\varepsilon}} - \dot{\lambda}\boldsymbol{m}), \tag{18}$$

whereby the auxiliary viscoplastic consistency condition

$$\dot{f} = \boldsymbol{n} : \boldsymbol{E} : \dot{\boldsymbol{\varepsilon}} - (\boldsymbol{n} : \boldsymbol{E} : \boldsymbol{m} - r)\dot{\lambda} + s\ddot{\lambda} = 0 \tag{19}$$

ensures continuous satisfaction of $f = 0$ under persistent viscous deformations.

We simplify Eq. (19) by assigning $a = \boldsymbol{n} : \boldsymbol{E} : \dot{\boldsymbol{\varepsilon}}$, $b = -(\boldsymbol{n} : \boldsymbol{E} : \boldsymbol{m} - r)$ and $c = s$. Substituting $p = \dot{\lambda}$, Eq. (19) leads to the first-order differential equation

$$\dot{f} = a + bp + c\dot{p} = 0. \tag{20}$$

It should be noted that in general $a = a(\dot{\boldsymbol{\varepsilon}}, \lambda)$, $b = b(\lambda)$ and $c = c(\lambda)$, i.e. the coefficients vary with the viscoplastic process. To extend the analytical treatment, we assume that

- the strain rate is constant, $\dot{\boldsymbol{\varepsilon}} = \text{const}$,
- a is a linear function of $\dot{\boldsymbol{\varepsilon}}$,
- b and c are constant.

These assumptions hold true for perfect viscoplasticity under constant strain rate conditions. The solution of the first-order differential equation (20)

$$p = C_0 \, \mathrm{e}^{-(b/c)t} - \frac{a}{b} \tag{21}$$

comprises an exponential decay term of the initial condition and the forcing term for strain control.

Considering that the over-stress at $t = t_0$ is greater than or equal to zero and is related to the viscoplastic multiplier rate by Eq. (5), the integration constant C_0 leads in general to the following expression for the viscoplastic multiplier:

$$p = \dot{\lambda} = \left(\dot{\lambda}_0 + \frac{a}{b}\right)\mathrm{e}^{-(b/c)t} - \frac{a}{b} \quad \text{with} \quad \dot{\lambda}_0 = \frac{\psi(F)_0}{\eta}. \tag{22}$$

The analytical solution of the viscoplastic multiplier $\dot{\lambda}$ provides the missing link to develop the viscoplastic material tangent operator. Following the reasoning of elastoplasticity, the governing constitutive equation results in

$$\dot{\boldsymbol{\sigma}} = \boldsymbol{E} : \left(\dot{\boldsymbol{\varepsilon}} - \left(\left(\dot{\lambda}_0 + \frac{a}{b}\right)\mathrm{e}^{-(b/c)t} - \frac{a}{b}\right)\boldsymbol{m}\right). \tag{23}$$

Rearranging the terms and substituting the previous expressions for a and b

$$\begin{aligned}\dot{\boldsymbol{\sigma}} &= \boldsymbol{E} : \dot{\boldsymbol{\varepsilon}} - \frac{\boldsymbol{E} : \boldsymbol{m} \otimes \boldsymbol{n} : \boldsymbol{E}}{\boldsymbol{n} : \boldsymbol{E} : \boldsymbol{m} - r}\left(1 - \mathrm{e}^{-(b/c)t}\right)\dot{\boldsymbol{\varepsilon}} - \dot{\lambda}_0 \boldsymbol{E} : \boldsymbol{m} \\ &= \boldsymbol{E} : \dot{\boldsymbol{\varepsilon}} - \frac{\bar{\boldsymbol{m}} \otimes \bar{\boldsymbol{n}}}{h_{\mathrm{vp}}}\left(1 - \mathrm{e}^{-(b/c)t}\right)\dot{\boldsymbol{\varepsilon}} - \dot{\lambda}_0 \boldsymbol{E} : \boldsymbol{m}, \end{aligned} \tag{24}$$

where h_{vp} is the viscoplastic modulus

$$h_{\mathrm{vp}} = \boldsymbol{n} : \boldsymbol{E} : \boldsymbol{m} - r \tag{25}$$

and $\bar{\boldsymbol{m}}$, $\bar{\boldsymbol{n}}$ are the contractions $\bar{\boldsymbol{m}} = \boldsymbol{E} : \boldsymbol{m}$, $\bar{\boldsymbol{n}} = \boldsymbol{n} : \boldsymbol{E}$. As its definition in Eq. (22) shows, $\dot{\lambda}_0$ represents the *jump* in the initial stress condition. In the case of a smooth viscoplastic strain history, when there is no jump in the initial condition, i.e. $\dot{\lambda}_0 = 0$, we obtain the tangential elasto-viscoplastic constitutive relation

$$\dot{\boldsymbol{\sigma}} = \boldsymbol{E}_{\mathrm{T}}^{\mathrm{vp}} : \dot{\boldsymbol{\varepsilon}} \quad \text{with } \boldsymbol{E}_{\mathrm{T}}^{\mathrm{vp}} = \left[\boldsymbol{E} - \frac{\bar{\boldsymbol{m}} \otimes \bar{\boldsymbol{n}}}{h_{\mathrm{vp}}}\left(1 - \mathrm{e}^{-(b/c)t}\right)\right], \tag{26}$$

where $\boldsymbol{E}_{\mathrm{T}}^{\mathrm{vp}}$ denotes the viscoplastic tangent material operator. Comparing with the elastoplastic tangent material operator $\boldsymbol{E}_{\mathrm{T}}^{\mathrm{ep}}$, it is apparent that $\boldsymbol{E}_{\mathrm{T}}^{\mathrm{vp}}$ is bounded by the elastic stiffness $\boldsymbol{E}$ for the instantaneous response and by the elastoplastic stiffness $\boldsymbol{E}_{\mathrm{T}}^{\mathrm{ep}}$ for the long term response. In other words,

$$\boldsymbol{E}_{\mathrm{T}}^{\mathrm{vp}} \to \begin{cases} \boldsymbol{E} & \text{for} \quad t \to 0, \quad \eta \to \infty, \\ \boldsymbol{E}_{\mathrm{T}}^{\mathrm{ep}} & \text{for} \quad t \to \infty, \quad \eta \to 0. \end{cases} \tag{27}$$

In the transient regime, $\boldsymbol{E}_{\mathrm{T}}^{\mathrm{vp}}$ varies smoothly between the instantaneous elastic stiffness $\boldsymbol{E}$ and the elastoplastic stiffness $\boldsymbol{E}_{\mathrm{T}}^{\mathrm{ep}}$ according to the exponential function $1 - \mathrm{e}^{-(b/c)t}$.

3. Algorithmic viscoplastic tangent operators

In this section, we review several implicit algorithmic viscoplastic material operators for advancing the solution in a finite time step $\Delta t = t_{n+1} - t_n$ with the objective to compare the main features of the different tangent operators. In the case of plasticity-like rate dependent formulations, the development of such a material operator requires the solution of the differential format of the consistency equation for the viscoplastic multiplier.

3.1. Algorithmic tangent of Perzyna viscoplasticity

Aside from the early proposals of gradient-based implicit time marching strategies (Argyris et al., 1981), Ju (1990) introduces an algorithmic viscoplastic tangent operator in the context of J_2-viscoplasticity, which was extended to other material models (Etse and Willam, 1999). Starting from the Euler–Backward linearization of the differential viscoplastic constitutive relations and expressing the incremental stress–strain relation in terms of the stress residual function, this operator can be expressed as

$$\boldsymbol{E}_{\mathrm{T}}^{\mathrm{p}} = \frac{\mathrm{d}\boldsymbol{\sigma}}{\mathrm{d}\boldsymbol{\varepsilon}} = \boldsymbol{E}^{\mathrm{p}} - \frac{\bar{\boldsymbol{m}}^{\mathrm{p}} \otimes \bar{\boldsymbol{n}}^{\mathrm{p}}}{\frac{\eta}{\bar{s}\Delta t} + \boldsymbol{n} : \boldsymbol{E}^{\mathrm{p}} : \boldsymbol{m}}, \tag{28}$$

where $\boldsymbol{M}$ is the Hessian of the viscoplastic potential $\boldsymbol{M} = \partial \boldsymbol{m} / \partial \boldsymbol{\sigma}$, $\bar{\boldsymbol{m}}^{\mathrm{p}}$ and $\bar{\boldsymbol{n}}^{\mathrm{p}}$ represent the tensor contractions $\bar{\boldsymbol{m}}^{\mathrm{p}} = \boldsymbol{E}^{\mathrm{p}} : \boldsymbol{m}$ and $\bar{\boldsymbol{n}}^{\mathrm{p}} = \boldsymbol{n} : \boldsymbol{E}^{\mathrm{p}}$, the fourth-order tensor $\boldsymbol{E}^{\mathrm{p}}$ is defined as

$$\boldsymbol{E}^{\mathrm{p}} = \left(\boldsymbol{E}^{-1} + \frac{\Delta t}{\eta} \psi(F) \boldsymbol{M} \right)^{-1}, \tag{29}$$

$$\tilde{s} = \frac{\partial \psi(F)}{\partial F}. \tag{30}$$

It has to be noted that $\boldsymbol{E}_{\mathrm{T}}^{\mathrm{p}}$ has the same structure as the elastoplastic tangent operator $\boldsymbol{E}_{\mathrm{T}}$ with $\boldsymbol{E}^{\mathrm{p}}$ playing the role of the elastic reference stiffness $\boldsymbol{E}$.

It follows that the time-dependent tangent operator $\boldsymbol{E}_{\mathrm{T}}^{\mathrm{p}}$ lead to the elastic operator as the quotient $\Delta t/\eta \to 0$. On the other hand for $\Delta t/\eta \to \infty$, the overstress measure tends to zero $\psi(F) \to 0$ and the value of $\boldsymbol{E}p$ is undefined. In consequence, the viscoplastic tangent operator does not approach the elastoplastic operator in the limit. In other words, $\boldsymbol{E}_{\mathrm{T}}^{\mathrm{p}}$ is bounded by

$$\boldsymbol{E}_{\mathrm{T}}^{\mathrm{p}} \to \begin{cases} \boldsymbol{E} & \text{for} \quad \Delta t \to 0, \quad \eta \to \infty, \\ \text{undefined} & \text{for} \quad \Delta t \to \infty, \quad \eta \to 0. \end{cases} \tag{31}$$

3.2. Algorithmic tangent material operator for continuous viscoplasticity

The introduction of a viscoplastic consistency condition in the framework of *continuous* or *consistent* viscoplasticity allows derivation of **algorithmic** tangent material operators. However, it is necessary to introduce an extra assumption concerning the second-order rate of the viscoplastic multiplier in the consistency condition. Truncated Taylor's series expansion in the form of $\dot{\lambda} = \Delta\lambda/\Delta t = \text{const}$ with $\ddot{\lambda} = 0$ has been proposed to eliminate the second derivative in the differential equation (17). This assumption is consistent with algorithmic linearization.

From the linearization of the backward Euler integration of the flow rule Eq. (5) and considering the time-step n, the viscoplastic strain increment is defined as

$$\Delta\boldsymbol{\varepsilon}_n^{\mathrm{vp}} = \Delta\lambda \boldsymbol{m} \tag{32}$$

Consequently, the incremental stress–strain relation and the internal variables increment read

$$\Delta\boldsymbol{\sigma}_n = \boldsymbol{E} : (\Delta\boldsymbol{\varepsilon} - \Delta\lambda \boldsymbol{m}), \tag{33}$$

$$\Delta q = h \Delta\lambda. \tag{34}$$

The differential format of the continuous viscoplastic consistency condition can be cast as

$$\mathrm{d}\bar{F} = \boldsymbol{n} : \mathrm{d}\boldsymbol{\sigma} + \frac{\partial \bar{F}}{\partial q}\, \mathrm{d}q - \frac{\partial \psi^{-1}(\dot{\lambda}\eta)}{\partial \dot{\lambda}}\, \mathrm{d}\dot{\lambda} = 0, \tag{35}$$

where the differential quantities are evaluated taking into account Eqs. (33) and (34), as $\mathrm{d}\boldsymbol{\sigma} = \boldsymbol{E}^m : (\mathrm{d}\boldsymbol{\varepsilon} - \mathrm{d}\Delta\lambda \boldsymbol{m})$, $\mathrm{d}q = h\, \mathrm{d}\Delta\lambda + \Delta\lambda \boldsymbol{p} : \boldsymbol{E}^m : (\mathrm{d}\boldsymbol{\varepsilon} - \mathrm{d}\Delta\lambda \boldsymbol{m})$ and $\mathrm{d}\dot{\lambda} = \mathrm{d}\Delta\lambda/\Delta t$. In those expressions, $\boldsymbol{E}^m = (\boldsymbol{E}^{-1} + \Delta\lambda \boldsymbol{M})^{-1}$ and $\boldsymbol{p} = \partial h(\boldsymbol{\sigma}, q)/\partial\boldsymbol{\sigma}$. Substituting into Eq. (35) and after some algebra

$$\mathrm{d}\Delta\lambda = \frac{(\boldsymbol{n} : \boldsymbol{E}^m + \Delta\lambda\, \bar{r}_{\mathrm{c}}\, \boldsymbol{p} : \boldsymbol{E}^m) : \mathrm{d}\boldsymbol{\varepsilon}}{\bar{h}_{\mathrm{vp}}^m + \bar{E}_i + \Delta\lambda \bar{E}_{\mathrm{p}}^m} \tag{36}$$

in which the following scalar definitions have been used

$$\bar{h}^m_{\rm vp} = \boldsymbol{n} : \boldsymbol{E}^m : \boldsymbol{m} - h\,\frac{\partial \bar{F}}{\partial q}, \tag{37}$$

$$\bar{E}^m_{\rm p} = \bar{r}_{\rm c}\,\boldsymbol{p} : \boldsymbol{E}^m : \boldsymbol{m}, \tag{38}$$

$$\bar{E}_i = -\frac{\bar{s}}{\Delta t}, \tag{39}$$

$$\bar{r}_{\rm c} = \frac{\partial \bar{F}}{\partial q}. \tag{40}$$

Substituting Eq. (36) into the tangential stress–strain relation $\mathrm{d}\boldsymbol{\sigma} = \boldsymbol{E}^{Ph}_{\rm Tc} : \mathrm{d}\boldsymbol{\varepsilon}$, the operator $\boldsymbol{E}^{Ph}_{\rm Tc}$ is the consistent tangent operator of continuous viscoplasticity

$$\boldsymbol{E}^{Ph}_{\rm Tc} = \boldsymbol{E}^m - \frac{\bar{\boldsymbol{m}}^m \otimes \bar{\boldsymbol{n}}^m}{\bar{h}^m_{\rm vp} + \bar{E}_i + \Delta\lambda \bar{E}^m_{\rm p}} - \Delta\lambda \frac{\bar{r}\,\bar{\boldsymbol{m}}^m \otimes \boldsymbol{p} : \boldsymbol{E}^m}{\bar{h}^m_{\rm vp} + \bar{E}_i + \Delta\lambda \bar{E}^m_{\rm p}}, \tag{41}$$

where $\bar{\boldsymbol{m}}^m = \boldsymbol{E}^m : \boldsymbol{m}$, $\bar{\boldsymbol{n}}^m = \boldsymbol{n} : \boldsymbol{E}^m$.

That is, $\boldsymbol{E}^{Ph}_{\rm Tc}$ is comprised by the fourth order tensor $\boldsymbol{E}^m$ degraded by two rate- and step-size dependent dyadic expansions. For the case $\Delta t \to 0$, the increment of the viscoplastic multiplier tends to zero $\Delta\lambda = \dot{\lambda}\Delta t \to 0$, then $\boldsymbol{E}^m \to \boldsymbol{E}$, and as $\bar{E}_i \to \infty$ this results in $\boldsymbol{E}^{Ph}_{\rm Tc} \to \boldsymbol{E}$. In the other limit when $\Delta t \to \infty$, this leads to the elastoplastic consistent tangent operator $\boldsymbol{E}^{Ph}_{\rm Tc} \to \boldsymbol{E}^{\rm ep}_{\rm Tc}$ as the rate dependent terms in the denominator and in $\bar{r}$ vanish. Then,

$$\boldsymbol{E}^{Ph}_{\rm Tc} \to \begin{cases} \boldsymbol{E} & \text{for} \quad \Delta t \to 0, \quad \eta \to \infty, \\ \boldsymbol{E}^{\rm ep}_{\rm Tc} & \text{for} \quad \Delta t \to \infty, \quad \eta \to 0. \end{cases} \tag{42}$$

Remark. *The original work of Ponthot* (1995) *did present a finite strain version of J_2 viscoplasticity model. In this work, the formulation was extended to a general hardening/softening non-associated viscoplasticity; however, for small strains.*

3.3. Tangent operator of consistent viscoplasticity

In this case, the differential viscoplastic consistency condition reads

$$\mathrm{d}\hat{F} = \boldsymbol{n} : \mathrm{d}\boldsymbol{\sigma} + \frac{\partial \hat{F}}{\partial q}\,\mathrm{d}q - \frac{\partial \hat{F}}{\partial \dot{q}}\,\mathrm{d}\dot{q} = 0 \tag{43}$$

with

$$\mathrm{d}\dot{q} = h\,\mathrm{d}\dot{\lambda} + \dot{\lambda}\,\boldsymbol{p} : \mathrm{d}\boldsymbol{\sigma} = \frac{h\,\mathrm{d}\Delta\lambda}{\Delta t} + \dot{\lambda}\,\boldsymbol{p} : \boldsymbol{E}^m : (\mathrm{d}\boldsymbol{\varepsilon} - \mathrm{d}\Delta\lambda \boldsymbol{m}). \tag{44}$$

Substituting Eq. (44) into the differential stress–strain relation together with the previous definitions of $\mathrm{d}\boldsymbol{\sigma}$ and $\mathrm{d}q$ and rearranging terms leads to

$$\mathrm{d}\Delta\lambda = \frac{(\boldsymbol{n} : \boldsymbol{E}^m + \Delta\lambda\,\hat{r}_{\rm c}\,\boldsymbol{p} : \boldsymbol{E}^m) : \mathrm{d}\boldsymbol{\varepsilon}}{\hat{h}^m_{\rm vp} + \hat{E}_i + \Delta\lambda \hat{E}^m_{\rm p}}, \tag{45}$$

where the following scalar definitions have been used

$$\hat{h}^m_{\rm vp} = \boldsymbol{n} : \boldsymbol{E}^m : \boldsymbol{m} - h\,\frac{\partial \hat{F}}{\partial q}, \tag{46}$$

$$\hat{E}^m_{\rm p} = \hat{r}_{\rm c}\,\boldsymbol{p} : \boldsymbol{E}^m : \boldsymbol{m}, \tag{47}$$

$$\hat{E}_i = \frac{\hat{s}}{\Delta t}, \tag{48}$$

$$\hat{r}_{\rm c} = \frac{\partial \hat{F}}{\partial q} + \frac{\hat{s}}{\Delta t}. \tag{49}$$

Eq. (45) into the discrete stress–strain relation lead to $\mathrm{d}\boldsymbol{\sigma} = \boldsymbol{E}^{\rm Wang}_{\rm Tc} : \mathrm{d}\boldsymbol{\varepsilon}$, where the consistent viscoplasticity operator $\boldsymbol{E}^{\rm Wang}_{\rm Tc}$ is

$$\boldsymbol{E}^{\rm Wang}_{\rm Tc} = \boldsymbol{E}^m - \frac{\bar{\boldsymbol{m}}^m \otimes \bar{\boldsymbol{n}}^m}{\hat{h}^m_{\rm vp} + \hat{E}_i + \Delta\lambda \hat{E}^m_{\rm p}} - \Delta\lambda\,\frac{\hat{r}_{\rm c}\,\bar{\boldsymbol{m}}^m \otimes \boldsymbol{p} : \boldsymbol{E}^m}{\bar{h}^m_{\rm vp} + \bar{E}_i + \Delta\lambda \bar{E}^m_{\rm p}}. \tag{50}$$

The differences between Eqs. (41) and (50) are the scalar quantities defined in Eqs. (40) and (49). Thus, the previous observations concerning the limit values of the continuous viscoplasticity operator remain valid for this case.

Remark. *Wang* (1997) *introduced consistent viscoplasticity in the context of small strain J_2 model. As the expressions presented here rely on general hardening/softening non-associated viscoplasticity, they lead to the same equations as Wang, when the J_2-model is considered.*

4. Exact solution of perfect J_2 viscoplasticity

The analytical solution of J_2 elastoplasticity was presented in a landmark paper by Krieg and Krieg (1977). The solution for perfectly plastic behavior was subsequently extended by Yoder and Whirley (1984) to hardening–softening J_2-elastoplasticity. In sequel, Loret and Prevost (1986) developed an analytical solution for hardening Drucker–Prager elastoplasticity.

Given the analytical solution for the viscoplastic multiplier rate in Eq. (22), we are able to obtain an exact solution for *continuous* and *consistent* viscoplasticity problems. In isotropic elasticity, the volumetric behavior decouples entirely from the deviatoric one, thus the volumetric stress is $\sigma^{\rm vol} = 3K\epsilon^{\rm vol}$, where K denotes the elastic bulk modulus and $\epsilon^{\rm vol}$ the volumetric strain. The deviatoric behavior is $\boldsymbol{s} = 2G\boldsymbol{e}$, where $\boldsymbol{s}$ and $\boldsymbol{e}$ are the deviatoric stress and strain tensors, respectively, and G is the shear modulus. In J_2 viscoplasticity only the deviatoric behavior is inelastic, i.e. $\boldsymbol{n} = \boldsymbol{m} = \boldsymbol{s}$, thus we confine our attention to the deviatoric stress–strain rate relation

$$\dot{\boldsymbol{s}} = 2G(\dot{\boldsymbol{e}} - \dot{\lambda}\boldsymbol{s}), \tag{51}$$

where the deviatoric viscoplastic strain rate is $\dot{\boldsymbol{e}}_{\rm vp} = \dot{\lambda}\boldsymbol{s}$. The rate-dependent J_2 yield criterion writes in the case of linear overstress behavior when $N = 1$

$$f(\boldsymbol{s}, \dot{\lambda}) = \frac{1}{2}\boldsymbol{s} : \boldsymbol{s} - \frac{y_0^2}{3}\left(1 + \frac{y_0}{\sqrt{3}}\eta\dot{\lambda}\right) = 0, \tag{52}$$

where y_0 denotes the yield stress in uniaxial tension, which is related to the yield strength in shear by $k = y_0/\sqrt{3}$ for continuous viscoplasticity. From the previous definitions, we find for $a = \boldsymbol{n} : \boldsymbol{E} : \dot{\boldsymbol{\varepsilon}} = 2G\boldsymbol{s} : \dot{\boldsymbol{e}}$, and for $b = -(\boldsymbol{n} : \boldsymbol{E} : \boldsymbol{m} - r) = -2G\boldsymbol{s} : \boldsymbol{s} + r$, and finally for $c = s = -k^3\eta$. The solution of the viscoplastic multiplier Eq. (22) reads then

$$\dot{\lambda} = \frac{a}{b}\left(e^{-(b/c)t} - 1\right) = \frac{\boldsymbol{s} : \dot{\boldsymbol{e}}}{\boldsymbol{s} : \boldsymbol{s}}\left(1 - e^{-\frac{2G\boldsymbol{s}:\boldsymbol{s}}{k^3\eta}t}\right). \tag{53}$$

Henceforth, Eq. (51) results in the differential equation

$$\dot{\boldsymbol{s}} = 2G\dot{\boldsymbol{e}} - 2G\frac{\boldsymbol{s} : \dot{\boldsymbol{e}}}{\boldsymbol{s} : \boldsymbol{s}}\left(1 - e^{-\frac{2G\boldsymbol{s}:\boldsymbol{s}}{k^3\eta}t}\right)\boldsymbol{s}, \tag{54}$$

which is a differential equation for the deviatoric stress $\boldsymbol{s}(t)$. It's interesting to note that Eq. (54) differs from the differential equation presented by Krieg and Krieg (1977) in the rate-dependent term $1 - e^{-(2G\boldsymbol{s}:\boldsymbol{s}/k^3\eta)t}$ affecting the inelastic deviatoric stress rate term.

Consider a stress state inside the elastic domain defined by the viscoplastic yield condition Eq. (52) at time $t = t_0$. During the time interval $\Delta t = t_f - t_0$, the deviatoric strain increment $\Delta\boldsymbol{e} = \dot{\boldsymbol{e}}\Delta t$ leads in the case of viscoplastic loading to the deviatoric stress increment $\Delta\boldsymbol{s}^e = 2G\Delta\boldsymbol{e}$ and to a trial stress outside the elastic domain. Thereby, the stress path reaches the yield surface at the contact point, $\Delta\boldsymbol{s}^c$, at time t_c. During the inelastic time interval $\Delta t^i = t_f - t_c$ the deviatoric stress evolves according to solution of the differential equation (54), which has two contributions, one drives the stress in the direction of deviatoric strain rate, and the other one in the direction of deviatoric stress.

4.1. Scalar format of deviatoric differential equation

Measuring the magnitude of shear stress in terms of the Westergaard parameter $\rho = \sqrt{\boldsymbol{s} : \boldsymbol{s}} = |\boldsymbol{s}|$, the inner product between the final deviatoric stress and the deviatoric strain rate may be written as

$$\boldsymbol{s} : \dot{\boldsymbol{e}} = |\boldsymbol{s}||\dot{\boldsymbol{e}}|\cos\Psi = \rho|\dot{\boldsymbol{e}}|\cos\Psi, \tag{55}$$

where Ψ is the angle between $\boldsymbol{s}$ and $\dot{\boldsymbol{e}}$ in the interval $0 \geqslant \Psi \geqslant \pi$. Following the argument of Krieg and Krieg $\dot{\boldsymbol{e}} = \text{const.}$, the time derivative reduces to

$$\frac{d(\boldsymbol{s} : \dot{\boldsymbol{e}})}{dt} = \dot{\boldsymbol{s}} : \dot{\boldsymbol{e}} = \dot{\rho}|\dot{\boldsymbol{e}}|\cos\Psi - \rho|\dot{\boldsymbol{e}}|\dot{\Psi}\sin\Psi. \tag{56}$$

Multiplying the viscoplastic material law equation (51) by $\dot{\boldsymbol{e}}$ to develop a scalar format by inner product operation, and taking into account Eq. (55) and the definition of ρ, we obtain with the help of trigonometric identities

$$\dot{\boldsymbol{s}} : \dot{\boldsymbol{e}} = 2G|\dot{\boldsymbol{e}}|^2(\sin^2(\Psi) + e^{-c_1\rho^2 t}\cos^2(\Psi)), \tag{57}$$

where $c_1 = 2G/k^3\eta$. Equating this expression with that for $\dot{\boldsymbol{s}} : \dot{\boldsymbol{e}}$ in Eq. (56)

$$\dot{\rho}\cos\Psi = 2G|\dot{\boldsymbol{e}}|(\sin^2(\Psi) + e^{-c_1\rho^2 t}\cos^2(\Psi)) + \rho\dot{\Psi}\sin\Psi. \tag{58}$$

Inner product operation of Eq. (51) with $\boldsymbol{s}$ and substituting $\boldsymbol{s} : \dot{\boldsymbol{s}} = 2\rho\dot{\rho}$, the scalar form of the shear stress rate may be expressed as

$$\dot{\rho} = \sqrt{2}G|\dot{\boldsymbol{e}}|e^{-c_1\rho^2 t}\cos\Psi. \tag{59}$$

From Eqs. (58) and (59), the viscoplastic evolution problem may be summarized as a system of two differential equations in $\dot{\rho}$, $\dot{\Psi}$:

$$\begin{aligned} \dot{\rho} &= c_0 e^{-c_1\rho^2 t}\cos\Psi \\ \dot{\Psi} &= -\tfrac{c_0}{\rho}\sin\Psi \end{aligned} \qquad \text{with } \rho(t_c) = \rho_c, \quad \Psi(t_c) = \Psi_c, \tag{60}$$

where $c_0 = 2G|\dot{\boldsymbol{e}}|$.

In sequel, we evaluate the analytical solution of Eq. (60) with the aid of a fourth-order explicit Runge–Kutta scheme, estimating the accuracy by comparing different time step results. In all cases, the error

estimator remained below 1×10^{-8}. Given, the solution Eq. (60) of the shear stress ρ and the angle Ψ it is still necessary to reconstruct the deviatoric stress state, which will be discussed in the next section.

Remark. *Perfect viscoplasticity introduces a rate dependent hardening–softening effect, thus the shear stress is no longer constant and* $\dot{\rho} \neq 0$ *must be considered in Eq.* (56). *In case of perfect plasticity, this term is zero and Eq.* (56) *together with Eq.* (57) *lead to the differential equation in* $\dot{\Psi}$ *presented by Krieg and Krieg* (1977).

4.2. Reconstruction of the tensor-valued solution

Multiplying both sides of Eq. (55) by the scalar $2G\Delta t^{i}$ leads to

$$\boldsymbol{s} : \Delta \boldsymbol{s}^{\text{trial}} = 2\rho \Delta \rho^{\text{trial}} \cos \Psi, \tag{61}$$

where $\Delta \boldsymbol{s}^{\text{trial}} = 2G\dot{\boldsymbol{e}}\Delta t^{i}$ is the deviatoric trial stress increment and $\Delta \rho^{\text{trial}} = |\Delta \boldsymbol{s}^{\text{trial}}|$ is the corresponding Westergaard shear increment. Under the assumption of constant strain rate and perfect viscoplasticity, Loret and Prevost (1986) showed that the solution of Eq. (54) is a linear combination of the form

$$\boldsymbol{s} = A\left(\boldsymbol{s}^{c} + B\Delta \boldsymbol{s}^{\text{trial}}\right), \tag{62}$$

where A and B are two scalar coefficients and $\boldsymbol{s}^{c} = \boldsymbol{s}^{0} + \Delta \boldsymbol{s}^{c}$. Applying Eqs. (52), (61) and (62) at the contact and the final states, the values of A and B may be written in terms of $\Delta \rho^{\text{trial}}$, ρ^{c}, ρ^{f}, Ψ^{c} and Ψ^{f} as

$$A = \frac{\rho^{f} \sin \Psi^{f}}{\rho^{c} \sin \Psi^{c}} \tag{63}$$

$$B = \frac{\rho^{c} \sin(\Psi^{c} - \Psi^{f})}{\Delta \rho^{\text{trial}} \sin \Psi^{f}} \tag{64}$$

It is important to note that in case of colinearity between $\boldsymbol{s}^{c}$ and $\Delta \boldsymbol{s}^{\text{trial}}$, the coefficients A and B reduce to simple scaling, where $A = \rho^{f}/\rho^{c}$ and $B = 0$. Also, due to the lack of an analytical form of this solution for the viscoplastic problem, the coefficients A and B are presented in terms of Ψ and ρ instead of the explicit expression for Ψ developed by Krieg and Krieg (1977). Table 1 summarizes the analytical viscoplastic solution.

5. Numerical results

This section presents results of the exact analytical reference solution to be compared with the results of different approximate algorithmic viscoplastic solutions described in the previous sections. We will compare the exact analytical solution with two algorithmic results for the test case of uniaxial tension of J_2 viscoplasticity in one-dimension and in plane strain. In addition to the study of the accuracy of the calculation, the localization predictions of the analytical viscoplastic operator are compared with the corresponding results of the algebraic viscoplastic operator considering simple shear of a Drucker–Prager material.

5.1. Uniaxial viscoplastic response

Fig. 1 shows the uniaxial test problem, the material properties and initial condition considered and the exact analytical stress history for different strain rates. The figure also depicts the uniaxial elastoplastic response (the rate independent case) for reference purposes. For zero strain rate, the test problem is the classical relaxation test for which the steady state response coincides with the elastoplastic one. As the

Table 1
Exact solution scheme for perfect J_2 viscoplasticity

- Elastic stress increment $\boldsymbol{s}^{\mathrm{e}} = \boldsymbol{s}^{0} + \Delta\boldsymbol{s}^{\mathrm{e}}$
- Check yield condition $F(\boldsymbol{s}^{\mathrm{e}}) > 0$, if holds
  - Check $F(\boldsymbol{s}^{0}) < 0$, if holds
    * Calculate contact time t_{c} and stress $\boldsymbol{s}^{\mathrm{c}}$ by secant method
  - else
    * Set $\boldsymbol{s}^{\mathrm{c}} = \boldsymbol{s}^{0}$, $t_{\mathrm{c}} = t_{0}$
  - Stress measures at contact point

$$\rho^{\mathrm{c}} = |\boldsymbol{s}^{\mathrm{c}}|,\ \Psi^{\mathrm{c}} = \arccos\left(\frac{|\boldsymbol{s}^{\mathrm{c}}||\dot{\boldsymbol{e}}|}{|\boldsymbol{s}^{\mathrm{c}} : \dot{\boldsymbol{e}}|}\right),\ \Delta\boldsymbol{s}^{\mathrm{trial}} = 2G\dot{\boldsymbol{e}}(t_{\mathrm{f}} - t_{\mathrm{c}})$$

  - RK4 solver for ρ^{f}, Ψ^{f} in *nsub* sub-increments:
    * Time sub-increment $\delta t = \frac{t_{\mathrm{f}} - t_{\mathrm{c}}}{nsub}$
    * Constants $c_0 = 2G|\dot{\boldsymbol{e}}|$, $c_1 = \frac{2G}{k^3\eta}$
    * Differential Functions:

$$\mathrm{d}\rho(c_0, c_1, \rho, \Psi, t) = c_0 \mathrm{e}^{-c_1\rho t}\cos\Psi$$

$$\mathrm{d}\Psi(c_0, c_1, \rho, \Psi, t) = -\frac{c_0}{\rho}\sin\Psi$$

    * for t in $[t_{\mathrm{c}}, t_{\mathrm{f}} - \delta t]$ step δt
      Calculate:

$$\rho_1 = \mathrm{d}\rho(c_0, c_1, \rho_t, \Psi_t, t),\ \ \Psi_1 = \mathrm{d}\Psi(c_0, c_1, \rho_t, \Psi_t, t)$$

$$\rho_2 = \mathrm{d}\rho(c_0, c_1, \rho_t + 0.5\rho_1,\ \ \Psi_t + 0.5\Psi_1, t + 0.5\delta t)$$

$$\Psi_2 = \mathrm{d}\Psi(c_0, c_1, \rho_t + 0.5\rho_1,\ \ \Psi_t + 0.5\Psi_1, t + 0.5\delta t)$$

$$\rho_3 = \mathrm{d}\rho(c_0, c_1, \rho_t + 0.5\rho_2,\ \ \Psi_t + 0.5\Psi_2, t + 0.5\delta t)$$

$$\Psi_3 = \mathrm{d}\Psi(c_0, c_1, \rho_t + 0.5\rho_2,\ \ \Psi_t + 0.5\Psi_2, t + 0.5\delta t)$$

$$\rho_4 = \mathrm{d}\rho(c_0, c_1, \rho_t + \rho_3,\ \ \Psi_t + \Psi_3, t + \delta t)$$

$$\Psi_4 = \mathrm{d}\Psi(c_0, c_1, \rho_t + \rho_3,\ \ \Psi_t + \Psi_3, t + \delta t)$$

$$\rho_{t+\delta t} = \rho_t + \frac{\delta t}{6}(\rho_1 + 2\rho_2 + 2\rho_3 + \rho_4)$$

$$\Psi_{t+\delta t} = \Psi_t + \frac{\delta t}{6}(\Psi_1 + 2\Psi_2 + 2\Psi_3 + \Psi_4)$$

    * Next t
    * $\rho^{\mathrm{f}} = \rho_t$, $\Psi^{\mathrm{f}} = \Psi_t$
  - Linear Combination Factors:

$$A = \frac{\rho^{\mathrm{f}}\sin\Psi^{\mathrm{f}}}{\rho^{\mathrm{c}}\sin\Psi^{\mathrm{c}}}\ B = \frac{\rho^{\mathrm{c}}\sin(\Psi^{\mathrm{c}} - \Psi^{\mathrm{f}})}{\rho^{\mathrm{trial}}\sin\Psi^{\mathrm{f}}}$$

  - Final deviatoric stress: $\boldsymbol{s}^{\mathrm{f}} = A(\boldsymbol{s}^{\mathrm{c}} + B\Delta\boldsymbol{s}^{\mathrm{trial}})$
- else
  - elastic increment or unloading: $\boldsymbol{s}^{\mathrm{f}} = \boldsymbol{s}^{\mathrm{e}}$

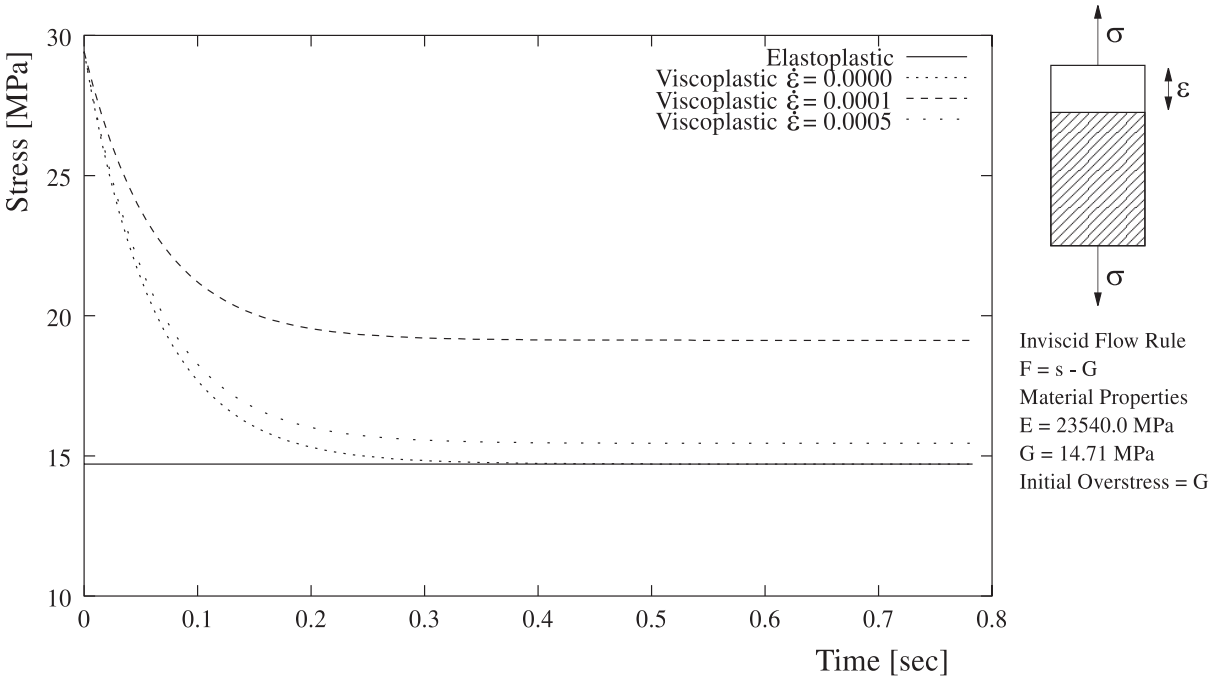

Fig. 1. Analytical viscoplastic stress histories in uniaxial tension ($\eta = 100$).

strain rate increases, the steady state stress response increases also. For the constant viscosity $\eta = 100$, the relaxation time remains constant and the duration of the transient regime does not change.

Fig. 2 compares the exact analytical with the algebraic viscoplastic stress histories for $\dot{\varepsilon} = 0.0005$. The algebraic viscoplastic solution was obtained with five increments. In the case of a single time step, the

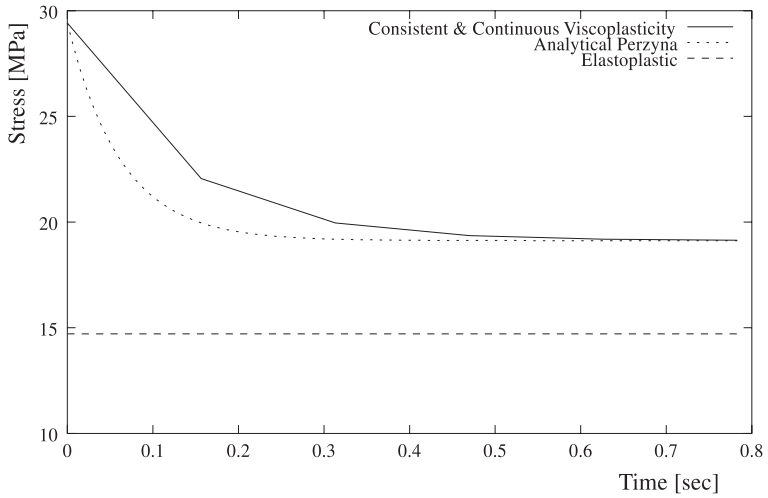

Fig. 2. Analytical and algorithmic viscoplastic stress histories in uniaxial tension for $\dot{\epsilon} = 0.0005$ and $\eta = 100$.

algebraic solution would coincide with the exact steady state solution, and as the number of time steps were increased, the differences in the transient regime would become smaller. In summary, there is no difference between the predictions of both the analytical and the algebraic solutions of the steady state response. On the other hand, the error in the transient regime diminishes with decreasing step size.

5.2. Error analysis of J_2 viscoplastic response in plane strain

Fig. 3 depicts the test setup and the axial load–displacement response using the exact analytical solution of continuous viscoplasticity for constant strain rate conditions in two-dimensional plane strain. For these numerical simulations, the material properties were $E = 23540$ MPa, $v = 0.3$ and the static yield strength of 14.71 MPa. All plots were obtained for the time interval $0 \leqslant t \leqslant 8.5 \times 10^{-4}$ s using 85 equal time-steps $\Delta t = 1.0 \times 10^{-5}$ s. As the viscosity η increases, the steady state result of the viscoplastic solution also increases. For comparison, the rate independent elastoplastic solution is shown together with the algebraic CPPM viscoplastic solution for $\eta = 10{,}000$. The error of the CPPM solution is, however, small both in the transient as well as in the steady state regime, when we consider the global response prediction. Thus, the question arises what the local errors are at the transition point from elastic to viscoplastic behavior and what the local errors are at steady state.

The error induced by the CPPM and the consistent linearization assumption $\dot{\lambda} = \Delta\lambda/\Delta t = \text{const.}$ is described by two error indicators. The first of them is the angle between the exact and the algebraic solutions, given by

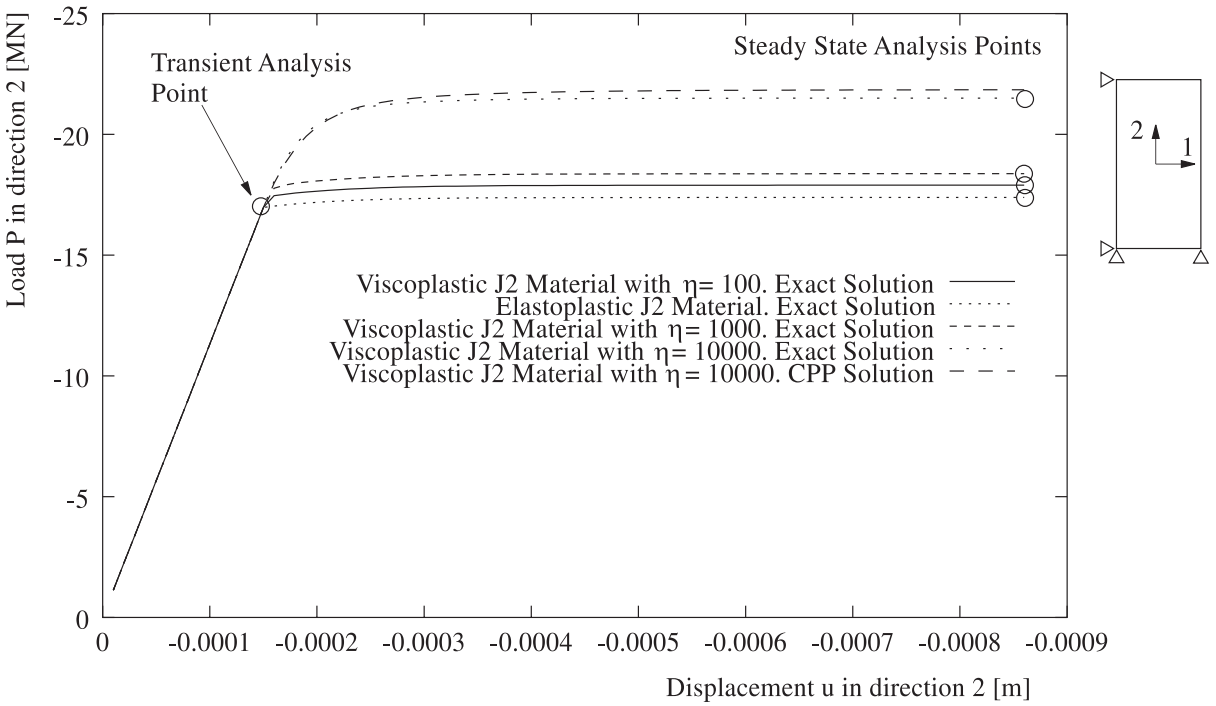

Fig. 3. Uniaxial compression test in plane strain: load–displacement diagrams.

$$\Psi_{\mathrm{err}} = \cos^{-1}\left(\frac{\boldsymbol{s}^{\mathrm{E}} : \boldsymbol{s}^{\mathrm{A}}}{|\boldsymbol{s}^{\mathrm{E}}||\boldsymbol{s}^{\mathrm{A}}|}\right). \tag{65}$$

The second one is the difference between the normalized shear stress parameters

$$E_l = 1 - \frac{\rho^{\mathrm{A}}}{\rho^{\mathrm{E}}}. \tag{66}$$

In these expressions, the superscripts A and E indicate algebraic and exact-analytical, respectively. The solution in the deviatoric plane can be described by its components in the direction of the normal $\boldsymbol{N}$ (normal direction) and the tangent to the yield surface $\boldsymbol{T}$ (tangential direction).

Figs. 4–9 present error maps of shear stress and angular distortions in the domain $(\boldsymbol{N}, \boldsymbol{T}) \in [0, 5\rho]; [0, 5\rho]$ at the two stages of analysis shown in Fig. 3 for $\eta = 100$ and $\eta = 10{,}000$. The angular elastoplastic error at the initial yield point and at the steady state response point does not show any significant differences and agrees with previous results (Krieg and Krieg, 1977). In the transition regime, we observe that the peak angular error does not vary significantly with the viscosity η, in fact, it is approximately 50% of the maximum elastoplastic angular error. As the viscosity parameter grows, the error maps are getting

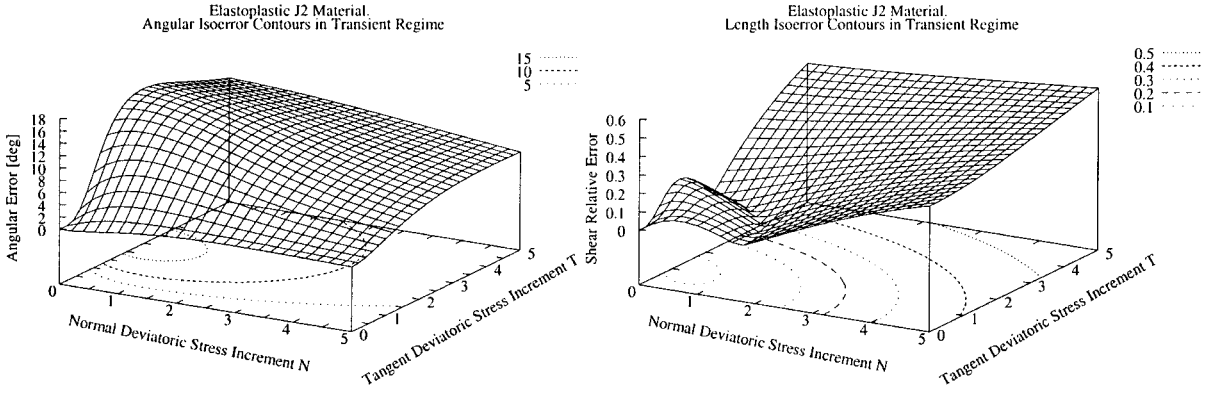

Fig. 4. Isoerror maps of shear magnitude and shear direction: elasto-plastic radial return solution at transition point.

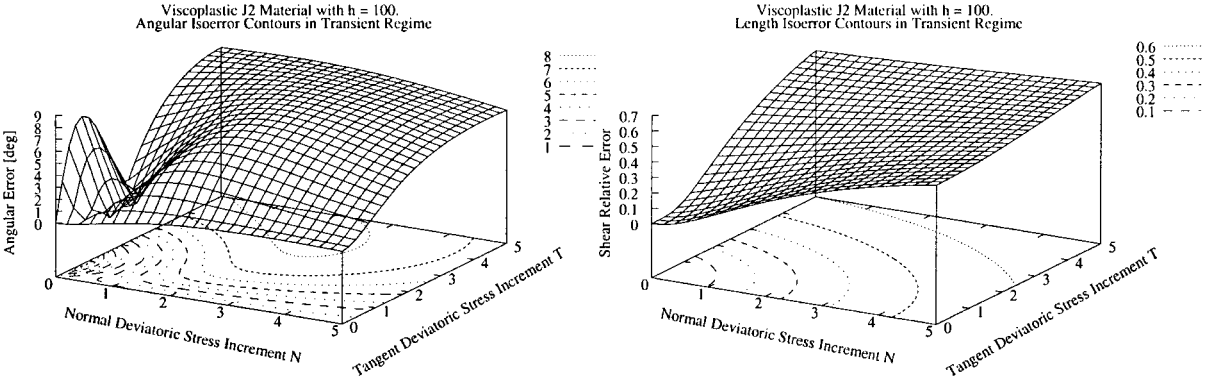

Fig. 5. Isoerror maps of shear magnitude and shear direction: continuous viscoplasticity radial return solution for viscosity $\eta = 100$ at transition point.

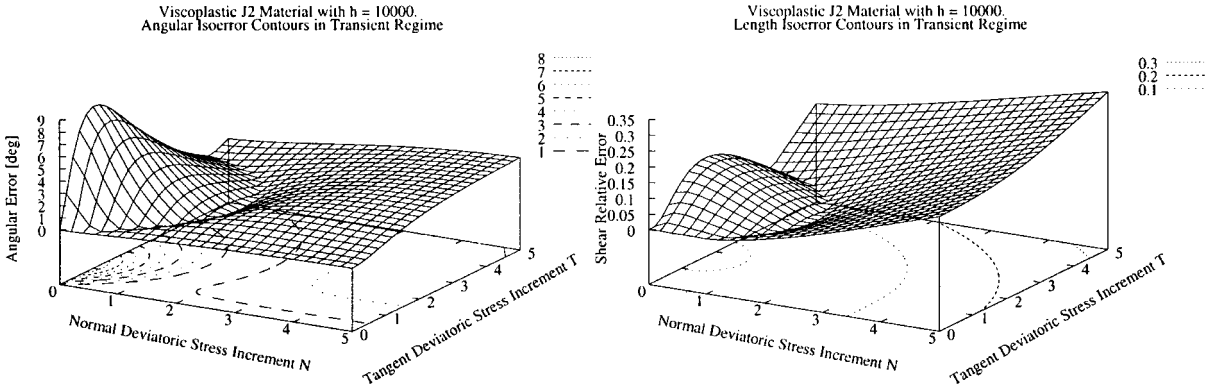

Fig. 6. Isoerror maps of shear magnitude and shear direction: continuous viscoplasticity radial return solution for viscosity $\eta = 10{,}000$ at transition point.

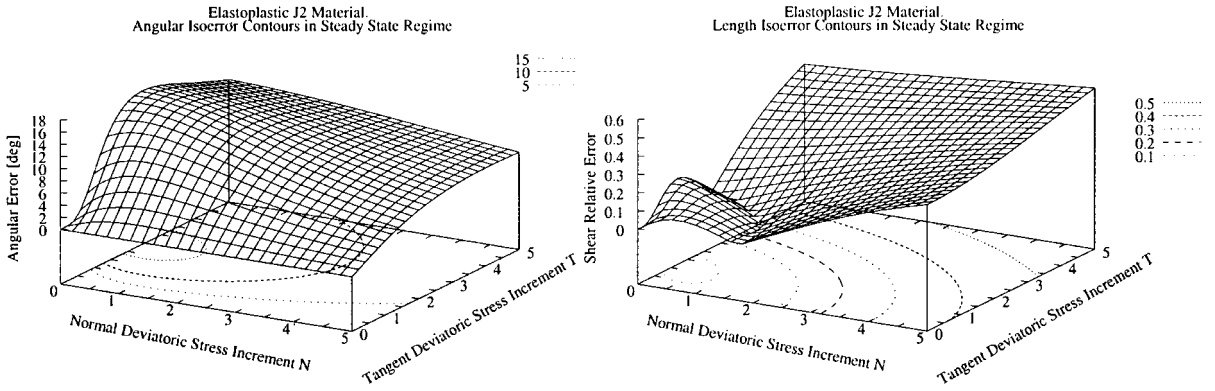

Fig. 7. Isoerror maps of shear magnitude and shear direction: elasto-plastic radial return solution at steady state.

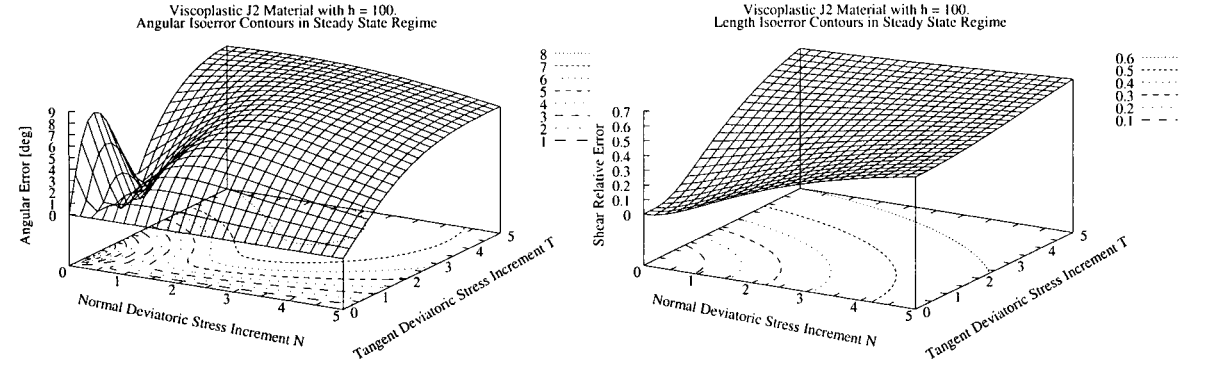

Fig. 8. Isoerror maps of shear magnitude and shear direction: continuous viscoplasticity radial return solution for viscosity $\eta = 100$ at steady state.

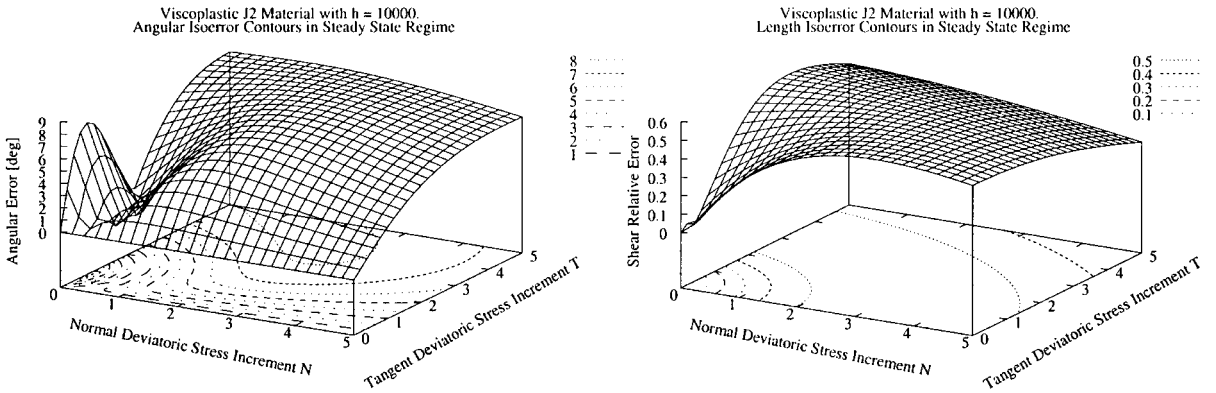

Fig. 9. Isoerror maps of shear magnitude and shear direction: consistent viscoplasticity radial return solution for viscosity $\eta = 10{,}000$ at steady state.

smoother. On the other hand, the shear stress error has the same general shape in all cases, it decreases as the rate dependency increases. This could be explained by the fact that both solutions have the same asymptotic limit, namely the elastic response for $\eta \to \infty$.

In the steady state regime, the maximum of the angular error is also constant, but there is no big difference in the shape of the isoerror map for the viscosities considered here. Another difference with the transient regime is that the shear stress error has almost the same maximum showing little deviation in the shape of the isoerror map. Despite the differences between steady state and transient regimes, the elastoplastic and viscoplastic isoerror maps clearly show that the influence of the assumption $\dot{\lambda} = \Delta\lambda/\Delta t = \text{const.}$ is negligible for all practical purposes. Moreover, the use of the viscoplastic CPPM diminishes the maximum shear stress error as much as 50% over the corresponding elastoplastic error.

The same error analysis is performed for classical Perzyna viscoplasticity. The constitutive integration of this model involves minimization of a stress or overstress function residuum. In this work, the latter strategy has been used. Figs. 10 and 11 show the angular and shear stress isoerror maps in the same $[\boldsymbol{N}, \boldsymbol{T}]$ domain as in the previous case. The angular isoerror map is similar in shape as the one obtained for the elastoplastic CPPM, with a maximum error, which is about twice of that of the consistent viscoplasticity

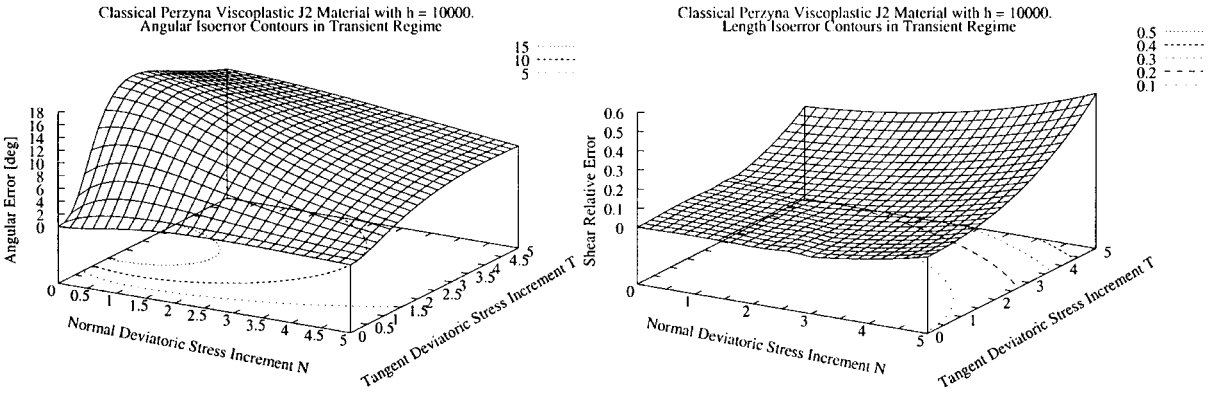

Fig. 10. Isoerror maps of shear magnitude and shear direction: classical viscoplasticity solution for viscosity $\eta = 10{,}000$ at transition point.

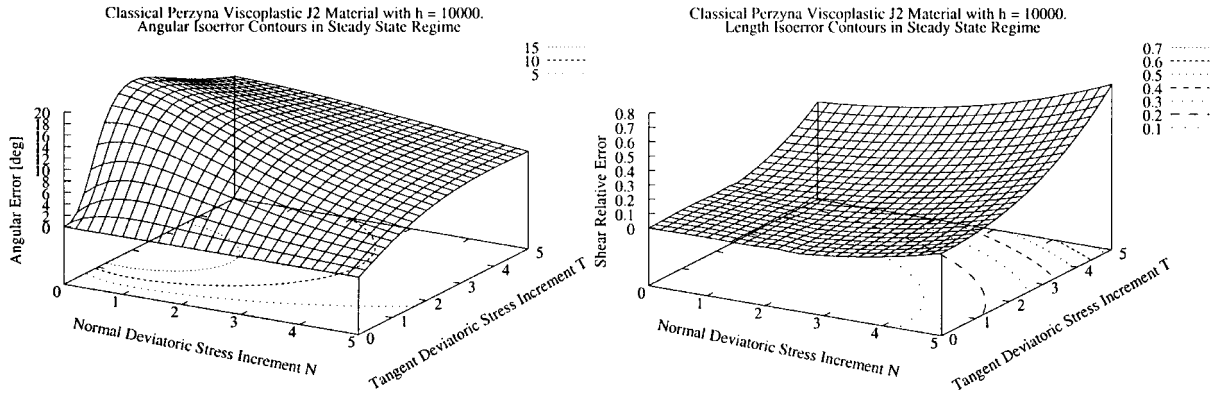

Fig. 11. Isoerror maps of shear magnitude and shear direction: classical viscoplasticity solution for viscosity $\eta = 10{,}000$ at steady state.

CPPM. Also, there is no significant difference between the error in the transient and in the steady state regime. The shear stress error remains of the same order as that of elastoplasticity and consistent viscoplasticity using CPPM.

5.3. Localization of Drucker–Prager viscoplasticity

In order to compare the predictions of the localized failure modes of the analytical and the algebraic viscoplastic tangent operators, we perform a simple shear test at the material level in the form of an equibiaxial compression-extension experiment. Fig. 12 shows the load–displacement plots for rate-independent

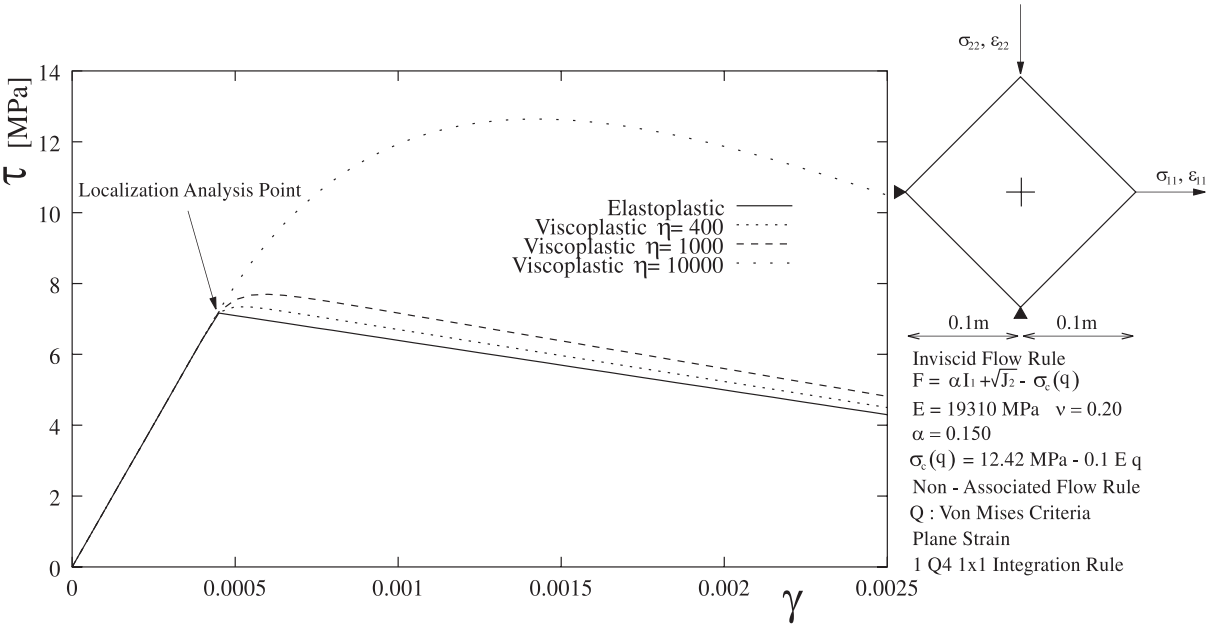

Fig. 12. Elastoplastic and continuous viscoplastic response under simple shear: nominal stress–strain diagram.

elastoplastic material behavior and for continuous viscoplasticity for different viscosity values $\eta = 400$, 1000 and 10,000. The figure summarizes the elastic and viscous softening properties considered and illustrates the effect of increasing viscosity on the strain softening response in simple shear.

Localization analysis of elastoplastic materials has been discussed extensively by Rudnicki and Rice (1975) and Ortiz et al. (1987), Runesson et al. (1991), Simo et al. (1993) among others. Its extension to viscoplastic behavior was examined by Needleman (1988), Loret and Prevost (1990), Willam et al. (1994), and recently by Etse and Willam (1999). Here, we adopt the normalized determinant of the tangent acoustic tensor $\det(\boldsymbol{Q}^{vp})/\det(\boldsymbol{Q})$ as a localization indicator. Thereby, the acoustic tensor is defined as $\boldsymbol{Q} = \vec{N}\boldsymbol{E}\vec{N}$, where $\vec{N}$ is the polarization vector, characterized by the angle θ between $\vec{N}$ and the coordinate axis $+\vec{1}$. Wave dispersion analysis (Sluys, 1992; Wang, 1997) constitutes a widely used alternative to the acoustic tensor analysis performed in this work.

Fig. 13 shows the localization predictions of the classical Perzyna viscoplastic tangent operator given by Eq. (28) at the point of transition from elasticity to viscoplasticity for the viscosity values in Fig. 12. We observe that for different values of η, the localization diagrams maintain the critical localization directions $\theta_{cr} = 40^\circ$ and $\theta_{cr} = 140^\circ$ of the elastoplastic operator. However, the material deterioration increases as the rate dependence diminishes (compare the plots for $\eta = 10{,}000$ and $\eta = 1000$). In contrast, close to the elastoplastic response, the lack of an asymptotic bound of the material operator leads to meaningless localization predictions ($\eta = 400$).

On the other hand, the localization diagrams of the algebraic viscoplastic tangent operator (Eq. (41)) shown in Fig. 14 exhibits smooth transition between the two limiting cases of elasticity and elastoplasticity. For comparison, Fig. 15 exhibits the localization predictions of the analytical viscoplastic tangent operator. The localization diagram shows the same critical direction $\theta_{cr} = 40^\circ$ as the previous algebraic tangent operator, but the degradation of the analytical tangent operator is far greater than that of the algebraic viscoplastic tangent operator. However, this large discrepancy diminishes for increasing values of the viscosity η, when both solutions are influenced more by the in common elastic contribution.

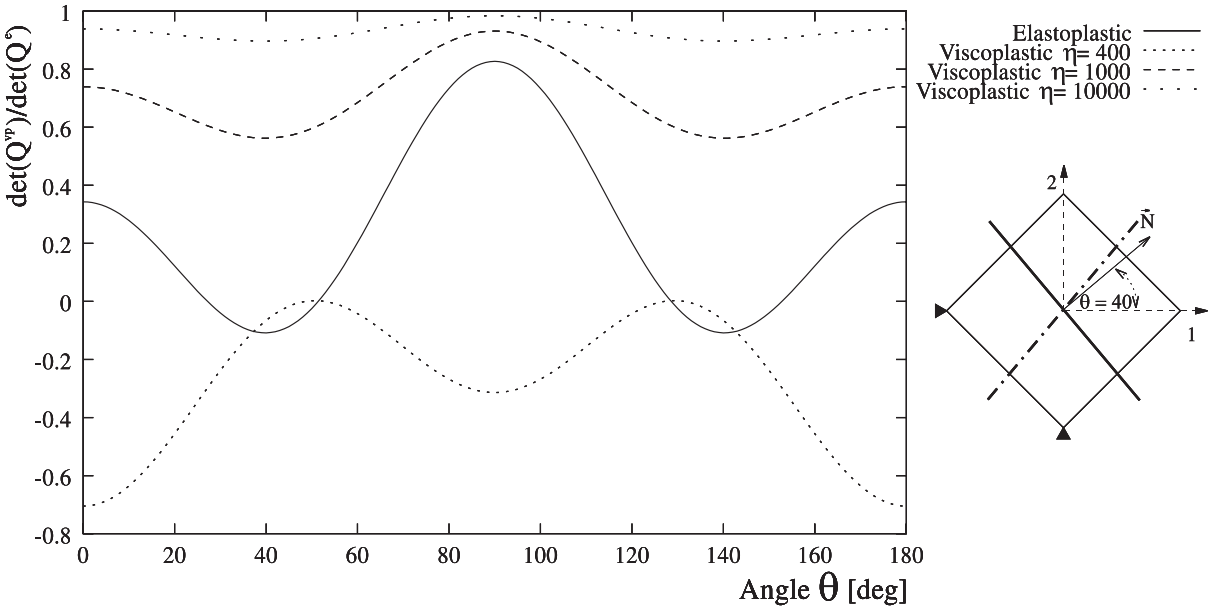

Fig. 13. Classical Perzyna viscoplasticity localization indicator for $\eta = 10{,}000$, $\eta = 1000$ and $\eta = 400$.

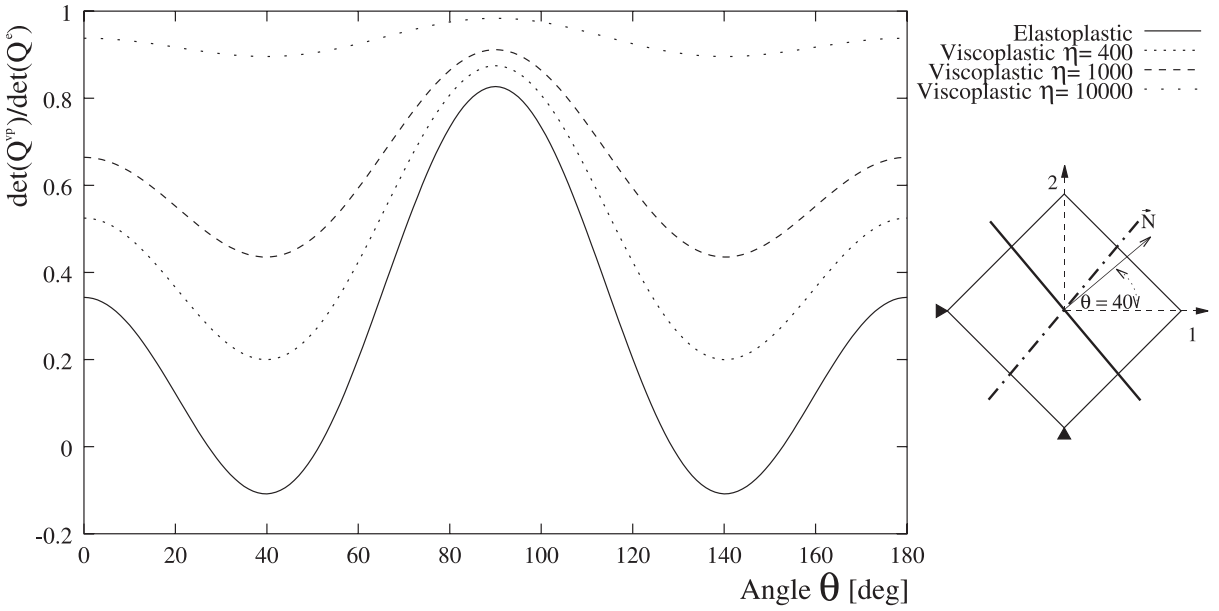

Fig. 14. Algebraic continuous viscoplasticity localization indicator for $\eta = 10{,}000$, $\eta = 1000$ and $\eta = 400$.

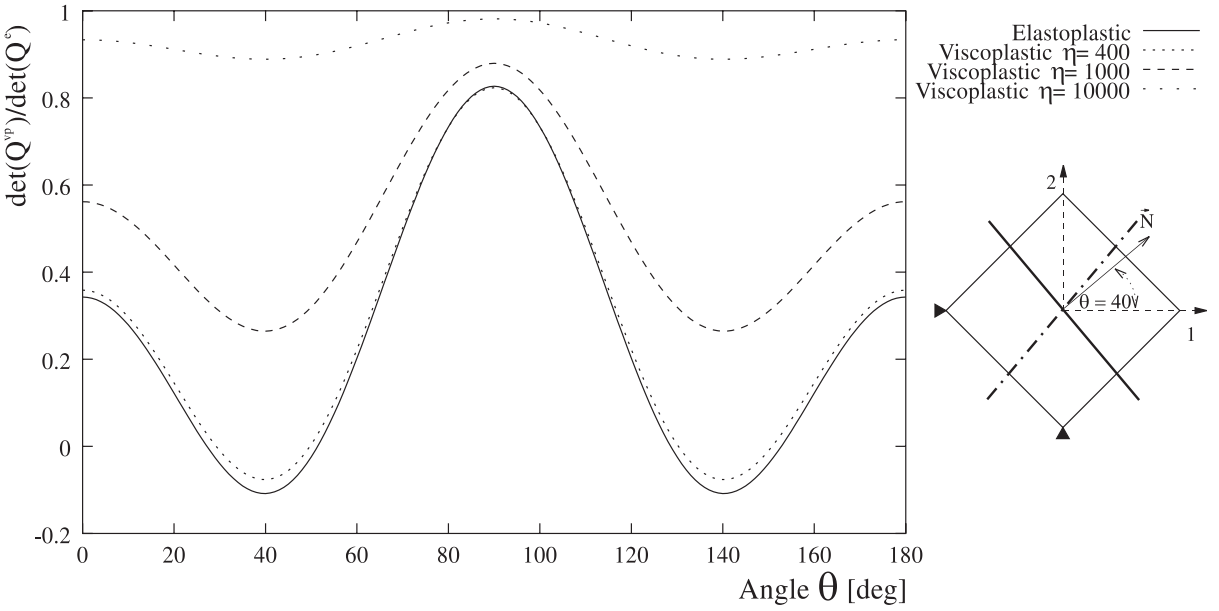

Fig. 15. Analytical viscoplasticity localization indicator for $\eta = 10{,}000$, $\eta = 1000$ and $\eta = 400$.

6. Conclusions

The results in this paper support the following conclusions:
(1) From the viscoplastic consistency condition defined by the plasticity-like rate dependent formulations, a differential tangential tensor can be obtained, which differs from the algorithmic operators defined so far.
(2) The assumption $\dot{\lambda} = \Delta\lambda/\Delta t = \text{const.}$ introduces errors of the same order of magnitude as the approximate algebraic constitutive integration strategy. In other terms, the algebraic approximation of $\ddot{\lambda} = 0$ in the viscoplastic multiplier introduces an error of the same order of magnitude as elastoplasticity, where the CPPM is widely used.
(3) The analytical viscoplastic tangent operator provides a smooth transition between the limiting cases of elastic and elastoplastic behavior. Also, the localization indicator predicts the same critical directions as the elastoplastic case and the algebraic viscoplastic tangent operator. However, the degradation of the localization indicator is significantly greater when the properties of the analytical acoustic tensor are compared with the corresponding algebraic operator.

Acknowledgements

The first and third author wish to thank the Argentine National Council of Scientifical and Technical Research CONICET. The second and first authors wish to thank the US National Science Foundation for the partial support of this effort under grant CMS-9634923 to the University of Colorado at Boulder. Opinions expressed in this paper are those of the writers and do not reflect those of the sponsors.

References

Argyris, J.H., Vaz, L.E., Willam, K.J., 1981. Integrated finite element analysis of coupled thermoviscoplastic problems. J. Thermal Stresses 4, 121–153.
Etse, G., Willam, K., 1999. Failure analysis of elastoplastic material models. J. Engng. Mech. 125, 60–69.
Ju, J.W., 1990. Consistent tangent moduli for a class of viscoplasticity. J. Engng. Mech. ASCE 116 (8), 1764–1799.
Krieg, R.D., Krieg, D.B., 1977. Accuracies of numerical solution methods for the elastic–perfectly plastic model. J. Pressure Vessel Tech. 99, 510–515.
Loret, B., Prevost, J.H., 1986. Accurate numerical solutions for Drucker–Prager elastic–plastic models. Comp. Meth. Appl. Mech. Engng. 54, 259–277.
Loret, B., Prevost, J.H., 1990. Dynamic strain localization in elasto- visco-plastic solids, Part 1. General formulation and one-dimensional examples. Comp. Meth. Appl. Mech. Engng. 83, 247–273.
Needleman, A., 1988. Material rate dependence and mesh-sensitivity in localization problems. Comp. Meth. Appl. Mech. Engng. 67, 69–85.
Ortiz, M., Leroy, Y., Needleman, A., 1987. A finite element method for failure analysis. Comp. Meth. Appl. Mech. Engng. 61, 189–214.
Perzyna, P., 1966. Fundamental problems in viscoplasticity. Adv. Appl. Mech. 9, 244–368.
Ponthot, J.P., 1995. Radial return extensions for visco-plasticity and lubricated friction. Proc. International Conference on Structural Mechanics and Reactor Technology SMIRT-13. Porto Alegre, Brazil, 2, 711–722.
Rudnicki, J.R., Rice J.W, 1975. Conditions for the localization of deformation in pressure-sensitive dilatant materials. J. Mech. Phys. Solids 23, 371–394.
Runesson, K., Ottosen, N.S., Peric, D., 1991. Discontinuous bifurcation of elastic–plastic solutions at plane stress and strain. Int. J. Plast. 5, 639–658.
Simo, J.C., Taylor, R.L., 1985. Consistent tangent operators for rate-independent elastoplasticity. Comp. Meth. Appl. Mech. Engng. 48, 101–118.
Simo, J.C., Oliver, J., Armero, F., 1993. An analysis of strong discontinuities induced by strain-softening in rate-independent inelastic solids. Comp. Mech. 12, 277–296.

Simo, J.C., Huges, T.J.R., 1998. Computational inelasticity. Interdiscipl. Appl. Math. Mech. Mat., Springer, New York.
Sluys, J.L., 1992. Wave propagation and dispersion in softening solids. Doctoral Thesis, TU-Delft, Netherlands.
Wang, W.M., 1997. Stationary and propagative instabilities in metals – a computational point of view. Doctoral Thesis, TU-Delft, Netherlands.
Wang, W.M., Sluys, J.L., de Borst, R., 1997. Viscoplasticity for instabilities due to strain softening and strain-rate softening. Int. J. Num. Meth. Engng. 40, 3839–3864.
Willam, K.J., Münz, T., Etse, G., Menetrey, P., 1994. Failure conditions and localization in concrete. In: N. Bicanic, R. de Borst, H. Mang (Eds.), Modeling of Concrete Structures. EURO-C, Pineridge, Swansea, pp. 263–282.
Winnicki, A., Pearce, C.J., Bicanic, N., 1998. Viscoplastic Hoffman model for concrete under dynamic loading. In: R. de Borst, N. Bicanic, H. Mang, Q. Meschke (Eds.), Computational Modelling of Concrete Structures. Balkema, Rotterdam, pp. 685–694.
Yoder, P.J., Whirley, B.G., 1984. On the numerical implementation of elastoplastic models. J. Appl. Mech. 51, 283–288.